

“Spatial Geotechnologies and GIS tools for urban planners applied to the analysis of urban heat island. Case Caracas city, Venezuela”
Contribution 115. GD8: New remote sensing Technology and data





“Spatial Geotechnologies and GIS tools for urban planners applied to the analysis of urban heat island. Case Caracas city, Venezuela” Contribution 115.
GD8: New remote sensing Technology and data





“Spatial Geotechnologies and GIS tools for urban planners applied to the analysis of urban heat island. Case Caracas city, Venezuela” Contribution 115. GD8: New remote sensing Technology and data

USGS Global Visualization ... x +

glovis.usgs.gov

Buscar

WRS-2 Path / Row: 4 53 Go

Lat/ Long: 10.1 -67.1 Go

Max Cloud: 100% [Left Arrow] [Up Arrow] [Down Arrow] [Right Arrow]

Scene Information:

ID: LC80040532015120LGN00

CC: 0% Date: 2015/4/30

Qty: 9 Product: OLI TIRS L1T

Apr 2015 Go

Prev Scene Next Scene

The main window displays a satellite image of Caracas, Venezuela. The image is a mosaic of several smaller images, showing a mix of green vegetation, brown urban areas, and dark water bodies. A yellow rectangular box highlights a specific area in the center of the image, which appears to be a mix of green and brown. The interface includes a map of South America on the left with a red dot indicating the location of Caracas. Below the map are controls for WRS-2 Path / Row, Lat/ Long, Max Cloud, and Scene Information.



“Spatial Geotechnologies and GIS tools for urban planners applied to the analysis of urban heat island. Case Caracas city, Venezuela” Contribution 115. GD8: New remote sensing Technology and data

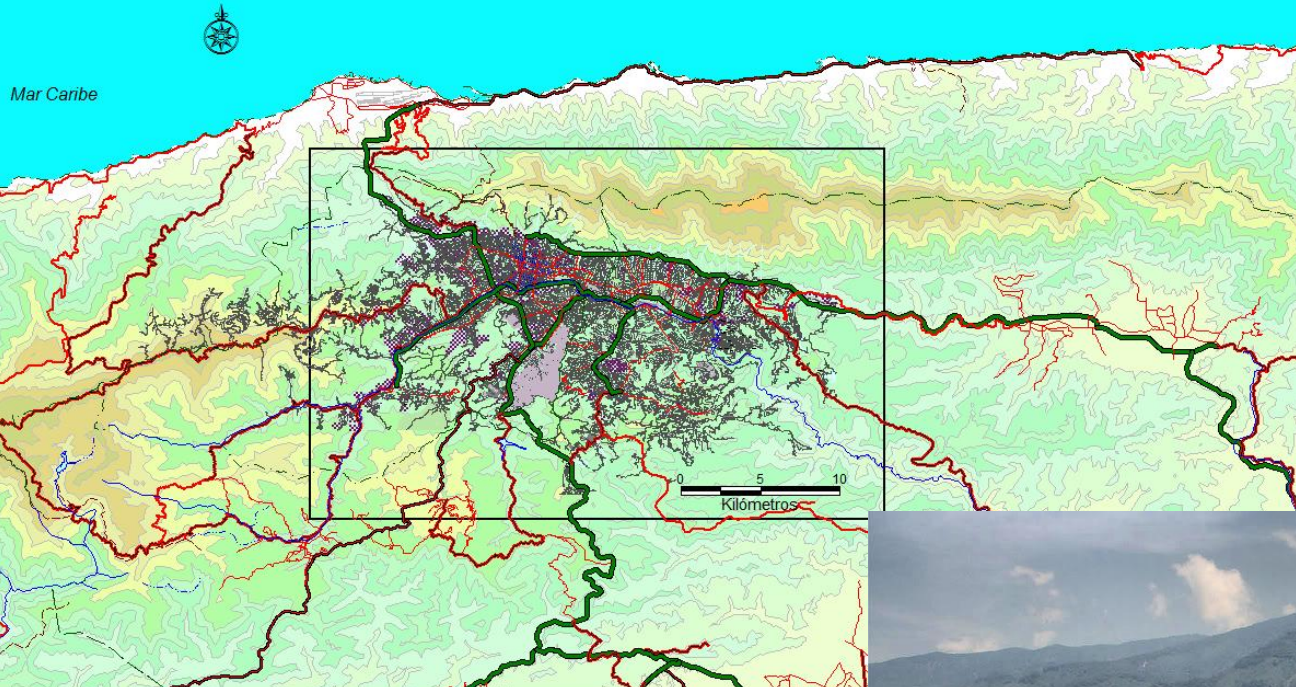


Fig.1

The city of Caracas, as many others Latin-American cities, has experimented a fast growth in the late 20 years, demographic pressures, and the lack of an appropriate urban planification, and others socio-economic problems, tend to reinforce the urbanization phenomena, that has transformed the environment, and the quality of life in these cities.

Geospatial tools has provide an interesting perspective to understand the dynamics of these phenomena, the use of thermal band to measure the extension an intensity of urban heat island has been used combined with terrestrial observations, to explain the changes in the urban surface patterns.

Combining radiometric, resampling and geometrics corrections techniques, and integrating this information into a GIS, it is possible to compare urban land use to urban surface temperature and identified urban heat critical areas, more accuracy.





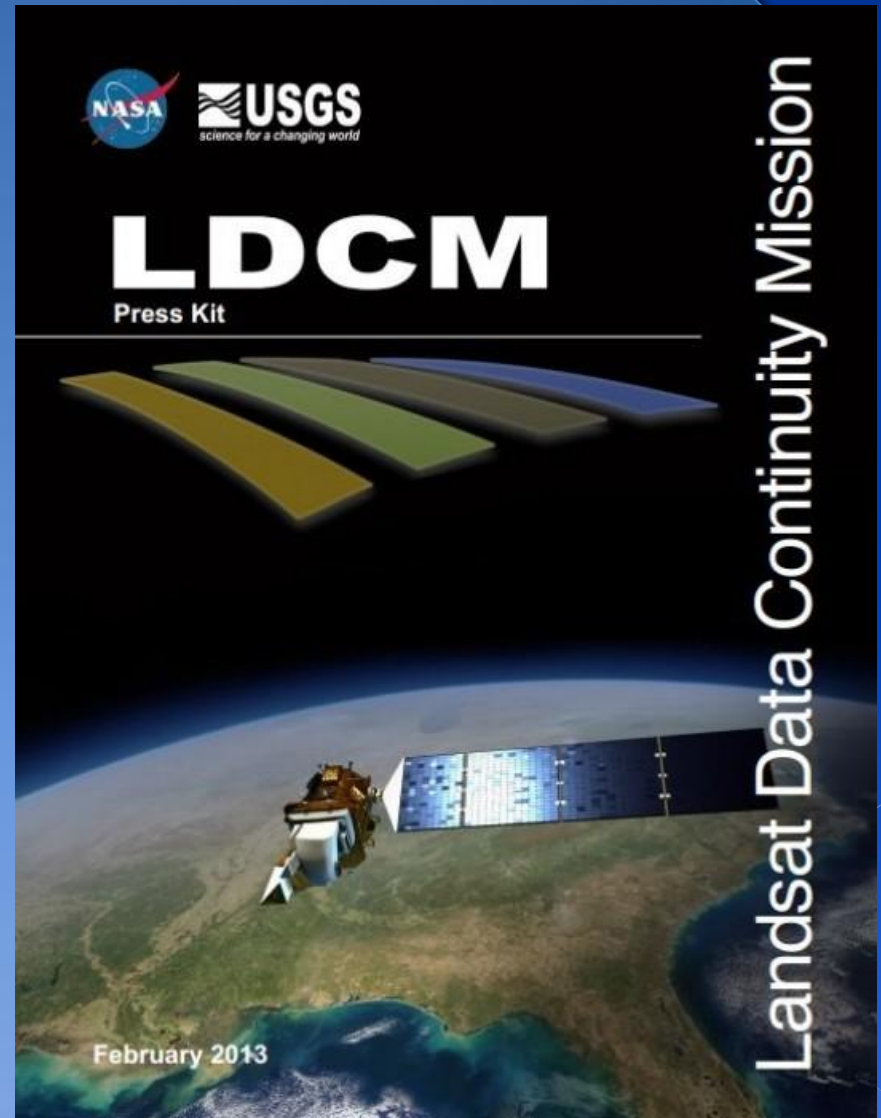
“Spatial Geotechnologies and GIS tools for urban planners applied to the analysis of urban heat island. Case Caracas city, Venezuela” Contribution 115. GD8: New remote sensing Technology and data

These works shows the result of the observations develops in the city of Caracas. The geospatial analysis was developed, using LANDSAT 8 OLI images for the period of selected, ERDAS 2014 for image processing, and ARC-GIS 10.3 for cartographic development.

Radiometric and Geometric correction (pixel by pixel) with ERDAS, allow us to work at city scales, in order to observe the variations in the urban canopy related to the urban surface temperatures patterns.

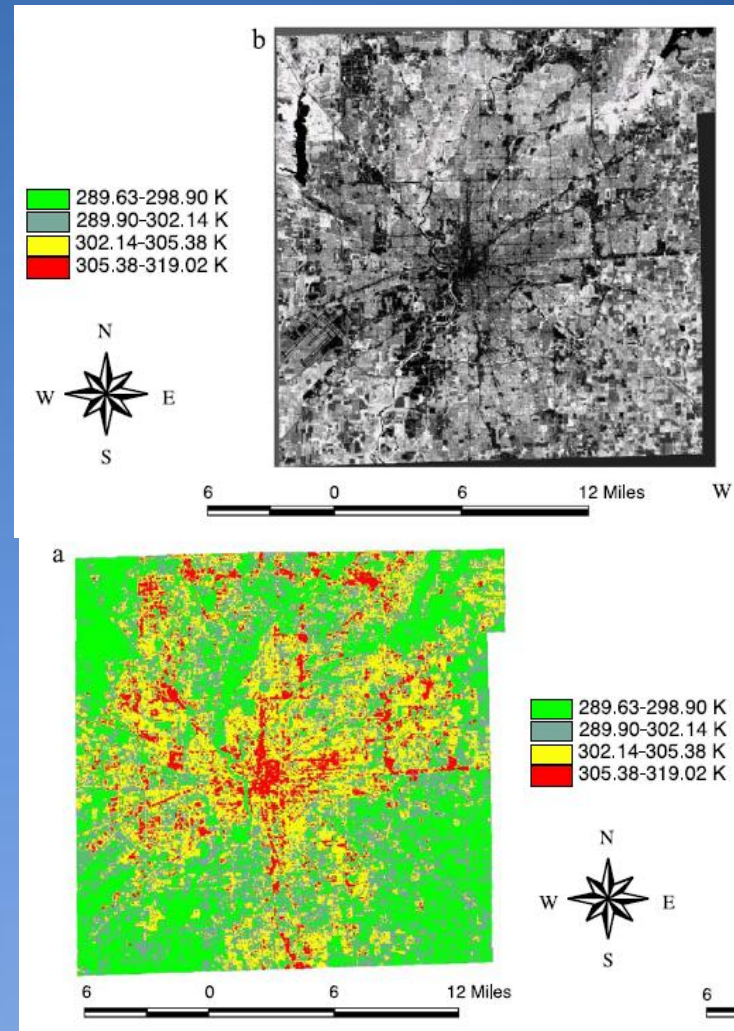
Results of the study were useful to identify critical areas and urban structures related to these thermal patterns.

This information will be use by urban planners, to develop mitigations and adaptation strategies, in order to prevent the intensification of the urban heat island, during the occurrence of an strong dry season, or heat waves, which might affect the city, the populations and the environment



2. Introduction

- Studies around the world of urban heat island phenomena using remote sensing techniques, have always **the limitations of the spatial resolution**, which may vary, depending on the period and the sensor selected for thermal analysis.
- For example, MODIS, AVHRR spatial resolution is around 1 km, ASTER 90 m, and LANDSAT 7 ETM +, **60 m**. These spatial resolution result particularly low for urban scales, even in the case of LANDSAT 7, one of the best original resolution available.
- Recently was launch **LANDSAT 8 OLI**, with an spatial resolution for thermal bands of 100 m, but resample to **30 m** for final users.
- These works shows the result of the geospatial analysis of the urban heat island phenomena in the city of Caracas.
- Combining radiometric and geometrics corrections with resampling techniques, and integrating this information into a GIS, allow us to work at to urban scales, to observe the variations in urban canopy related to the urban surface temperatures patterns.



3.1 Methodology and Materials.

Data source and processing:

- ❖ In this study, **Landsat-8 L1T** data provided by USGS with a track number LC8004053 was acquired in 2013-11-18, with a temporal resolution of 16-days.
- ❖ **Landsat-8 TIRS** is one of the most accurate thermal infrared sensors with relatively high spatial resolutions at present.
- ❖ It has the capability to acquire information in two **thermal infrared spectral bands of 10.90 and 12.0 μm** . Landsat 8 TIRS (Thermal Infrared Sensor) Band 10 and 11 and OLI (Operational Land Imager). **Thermal constant K1 and K2** and other image statistic are obtain from metadata of the image file.
- ❖ For data preprocessing, four procedures were implemented with ERDAS IMAGINE 2014 and ARC GIS 10.3.
- ❖ **First**, radiometric calibration and atmospheric correction were made to the OLI imagery. In this procedure, Digital Number (DN) values recorded by the sensor were converted into apparent reflectance and satellite brightness temperature for OLI-TIRS.
- ❖ **Second**, TIRS bands resampled in a 30-m resolution were reprojected from UTM/WGS1984 to LAT/LONG/WGS84, third, TIRS bands converted were integrated into a GIS with vectorial layers, of some relevant political and spatial information and finally NDVI analysis was done to compare LST patterns with NDVI results.

- *Temperature from TIRS:*
- The thermal TIRS bands 10 and 11 can be used to compute brightness temperature from radiance by inverting the Planck function.
- First of all, we need to convert the original DNs of TIRS into Top of Atmospheric Radiance (TOAr). Therefore, the original digital numbers (DN) of Landsat 8 TIR bands are converted into radiance based on the methods provided by Chander and Markham (2003) and the Landsat 8 Science Data Users Handbook (2015).
- The following equation 1 is used to convert original DNs into TOAr as shown below:
- $\text{TOAr} = M * \text{DN} + B$ (eq.1)
- Where: M is the Radiance Multiplier and B is the Radiance Add
- The M, B values are in the metadata file of Landsat 8 data. The radiometric calibration of thermal band 10 and Landsat 8 was done using following K1, K2 constants:
- Metadata of Landsat 8- **TIR-Band 10**
- Radiance Multiplier(M) 0.0003342
- Radiance Add(B) 0.1
- **K1** **774.89**
- **K2** **1321.08**

After we have got the TOAr values, TIRS band data can be converted from spectral radiance to brightness temperature, equation 2 (Landsat 8 Science Data Users Handbook, 2015) using the thermal constants provided in the metadata file:

$$T = \frac{K2}{\ln(K1 + 1)} \quad (\text{eq. 2})$$

where:

T = At-satellite brightness temperature (K)

λ = TOA spectral radiance (Watts/($\text{m}^2 \cdot \text{srad} \cdot \mu\text{m}$))

$K1$ = Band-specific thermal conversion constant from the metadata ($K1_CONSTANT_BAND_x$, where x is the band number, 10 or 11)

$K2$ = Band-specific thermal conversion constant from the metadata ($K2_CONSTANT_BAND_x$, where x is the band number, 10 or 11).

By using $K1$ and $K2$ parameters, we have converted the TOAr values into temperature in degrees kelvin. After this stage, we need to convert the unit of the temperature values into Fahrenheit or Celsius. This can be done by subtracting 273.15 from the degrees kelvin.

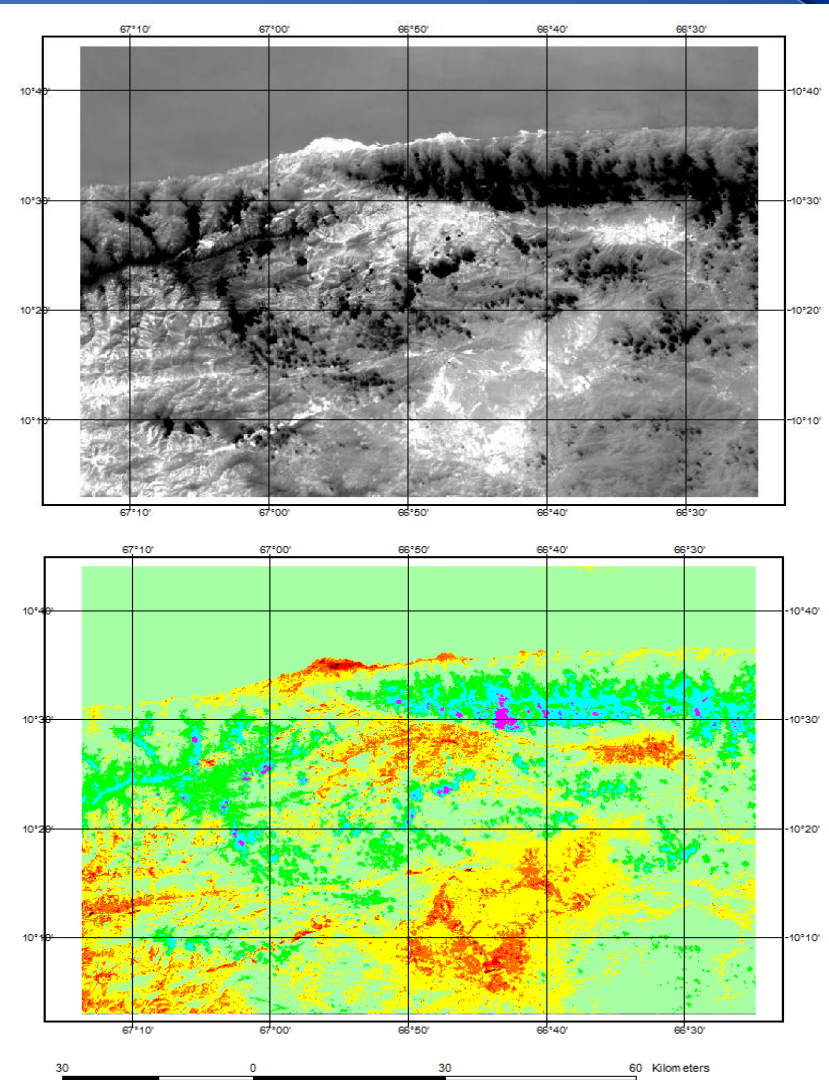
Though Landsat 8 TIRS has two thermal bands (10 and 11), only data from Band 10 are suitable at the moment for LST retrieval, due to the larger uncertainty in the Band 11 values (Barsi, J.A et al, 2014). Therefore, it was necessary to use a mono-window algorithm in the following form for LST retrieval from the Landsat 8 TIRS Band 10 data (Wang, F et al, 2015):

$$T_s = [a10(1 - C10 - D10) + (b10(1 - C10 - D10) + C10 + D10)T10 - D10Ta]/C10$$

where:

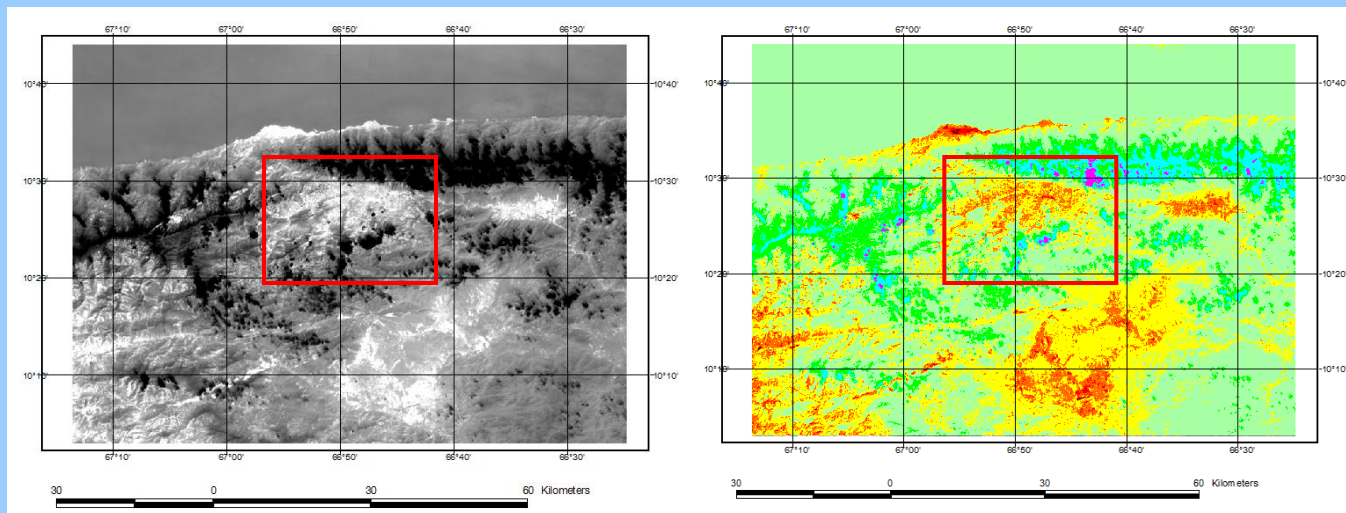
T_s is the LST retrieved from the Landsat 8 TIRS Band 10 data; T_a is the effective mean atmospheric temperature; $T10$ is the brightness temperature of Landsat 8 TIRS Band 10; $a10$ and $b10$ are the constants used to approximate the derivative of the Planck radiance function (Wang, F et al, 2015).

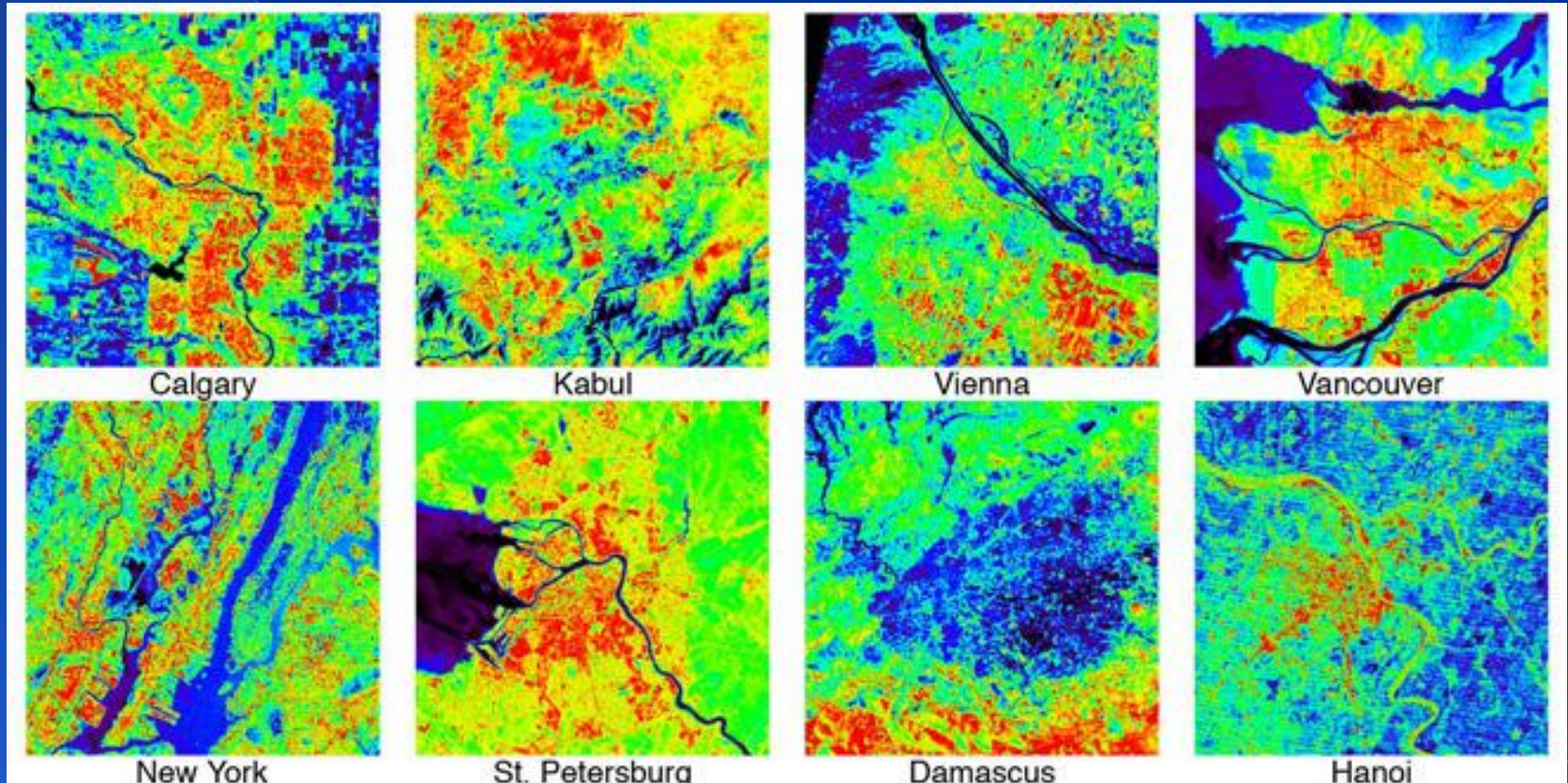
After complete the radiometric calibration and atmospheric correction, geometric corrections were developed in order to reproject the TIRS bands resampled in a 30-m resolution, from UTM /WGS 1984 to LAT /LONG /WGS84 to match the vectorial layer availables.



3.2 . Results and discussion

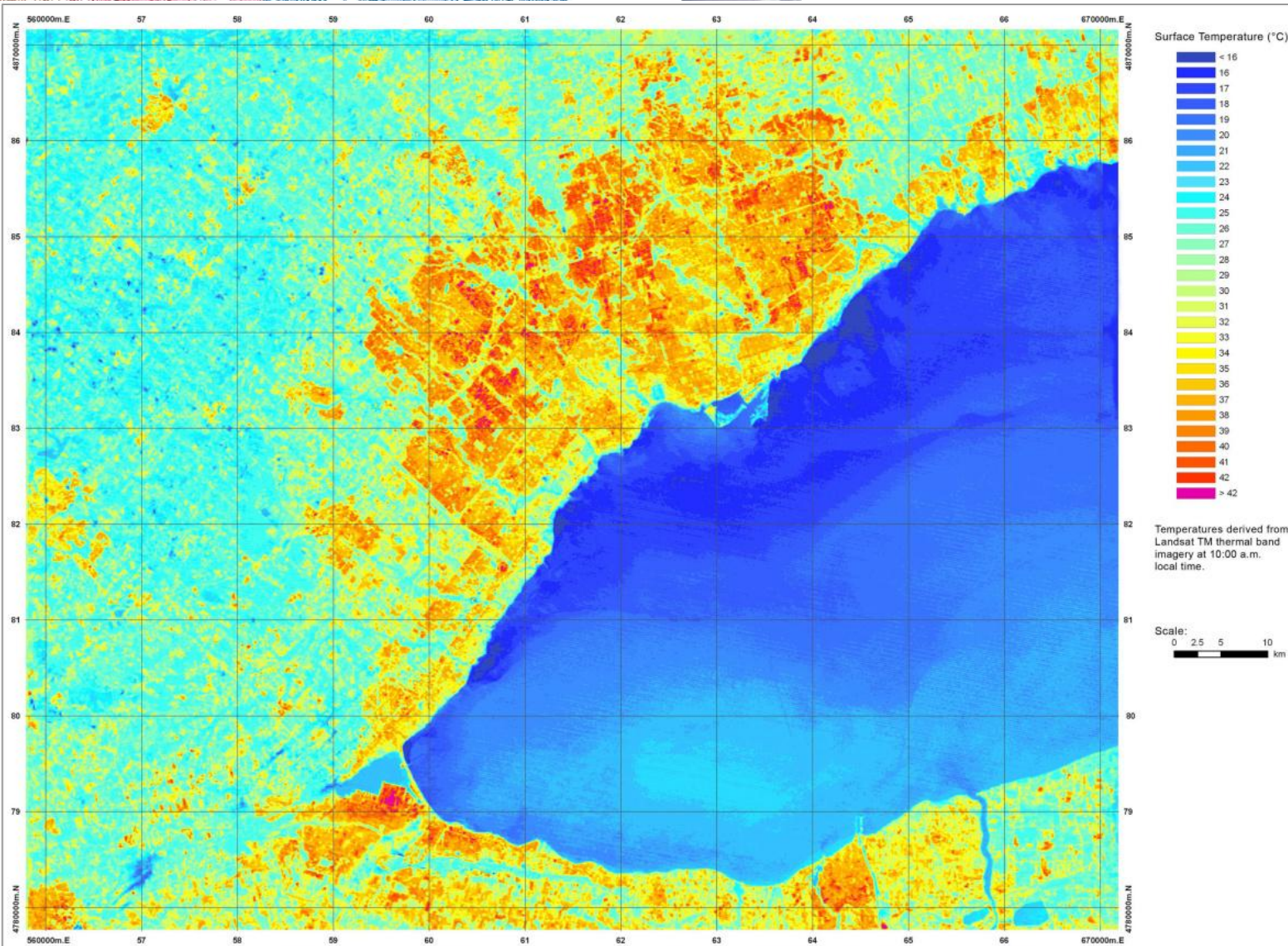
- GIS data, such as topographic variables, were first integrated in remote sensing natural mapping studies, because satellite data did not provide sufficient detail for effective management resource (Rogan, J., Miller, J., Wulder, M. A., & Franklin, S. E., 2006).
- The same happen in the case of urban climate studies, remote sensing did not provide sufficient detail for effective management for urban planners.
- Traditional studies about heat urban island has low spatial resolution, that barely shows the urban sprawl phenomena, and general differences in LST between urban and peri urban areas (Fig.2).
- Fig.2 Metropolitan area of Caracas city. Low spatial resolution, (a) B10 Landsat 8, (b) and LST. Red square shows the resample area.**





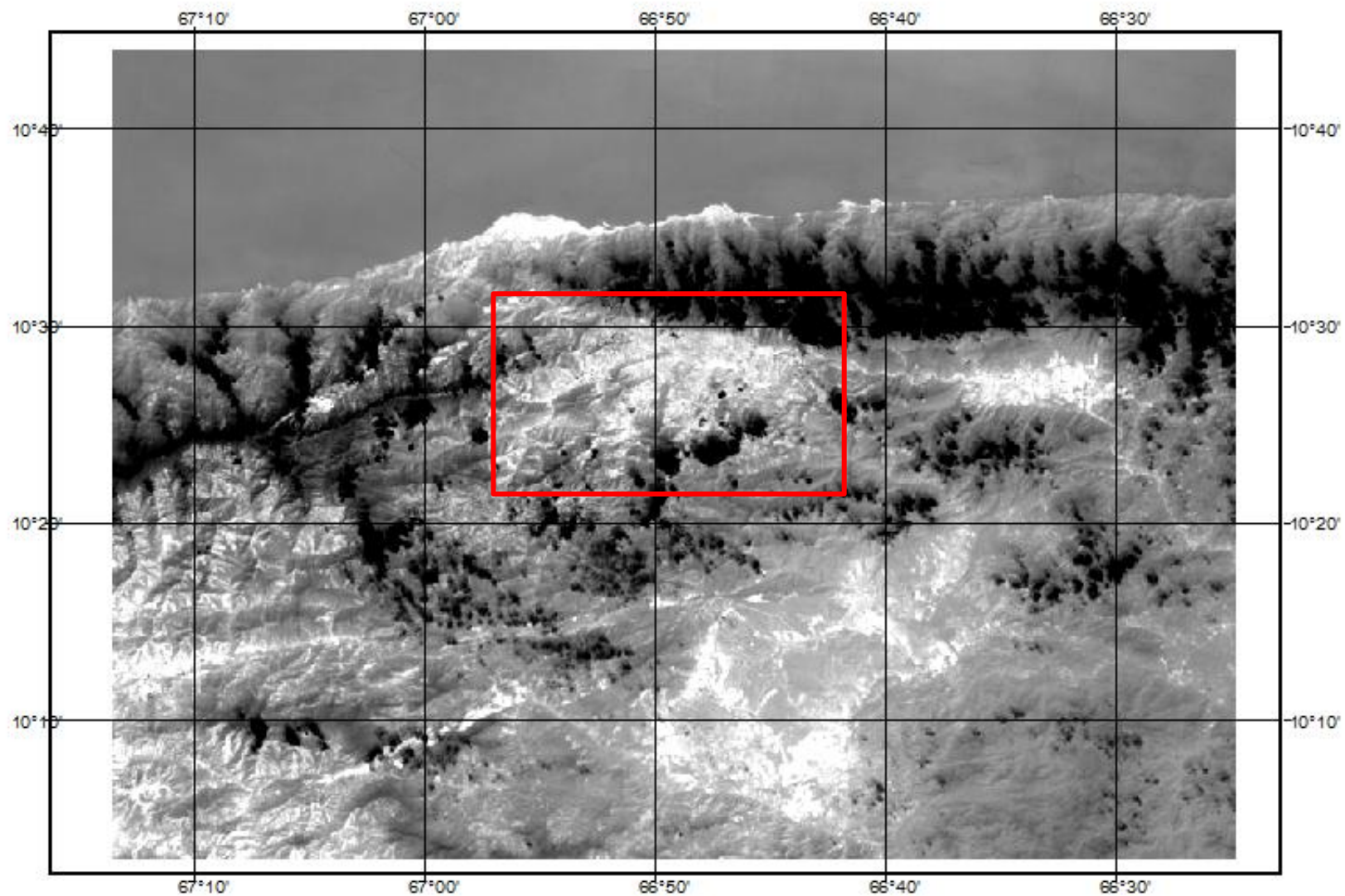
Comparative analysis of Landsat 7 ETM+ surface temperature for 24 cities shows, consistent relationships between surface temperature and vegetation. (Small, 2006).

Low spatial resolution studies.



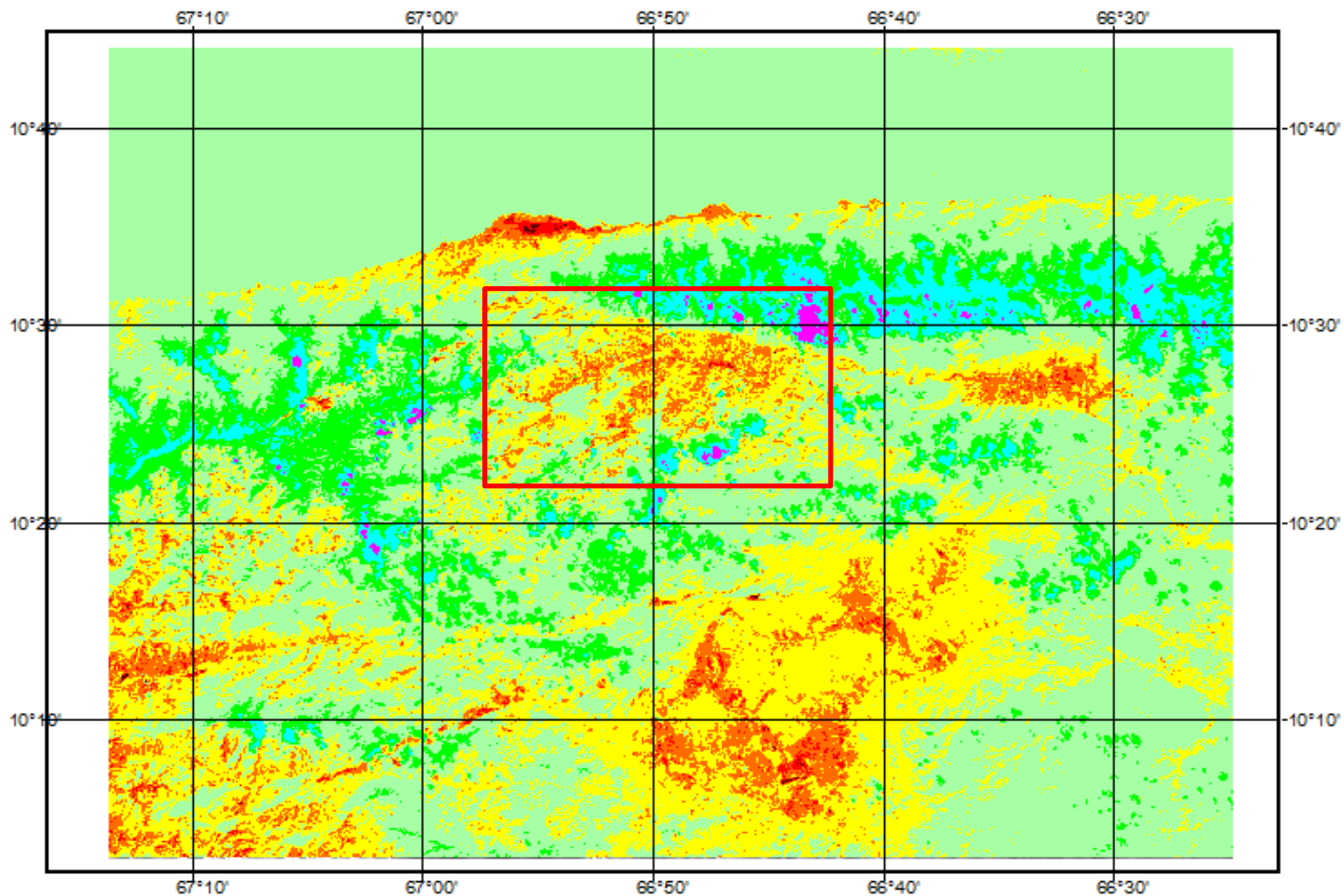
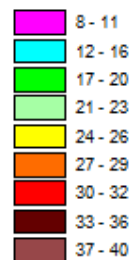
Land Surface Temperatures for the Greater Toronto Area, July 7, 2010

Médium resolution studies



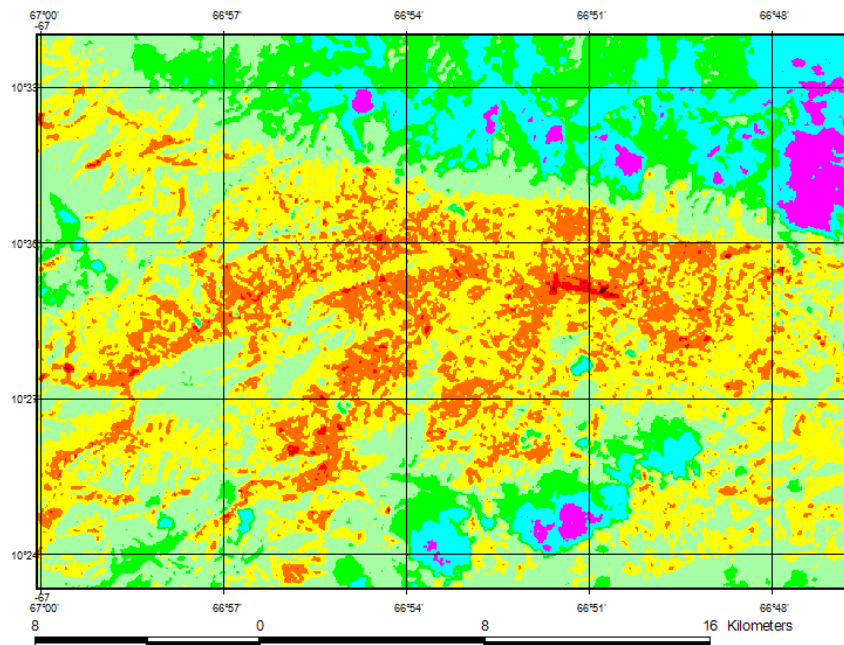
30 0 30 60 Kilometers



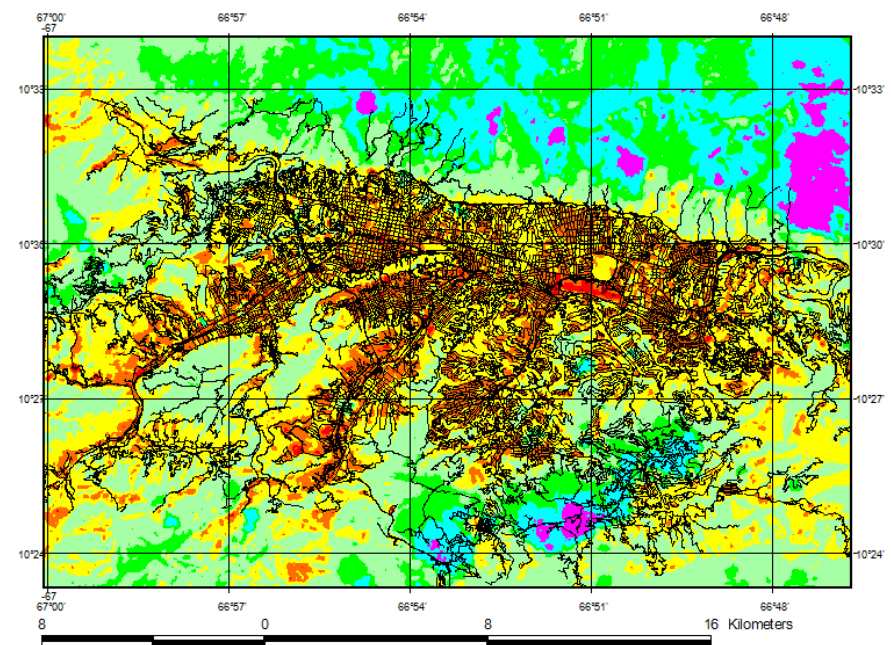


Using geometric and resampling techniques, and integrating this information into a GIS (Fig.3), it is possible to increase the information recover in the LST analysis. This method allows urban planner to visualize and understand the differences between urban sectors, and associate these differences to urban land use and urban construction materials.

Fig. 3 Example of GIS showing resampled area (a) and with vectorial layers of city streets in Caracas city(b).

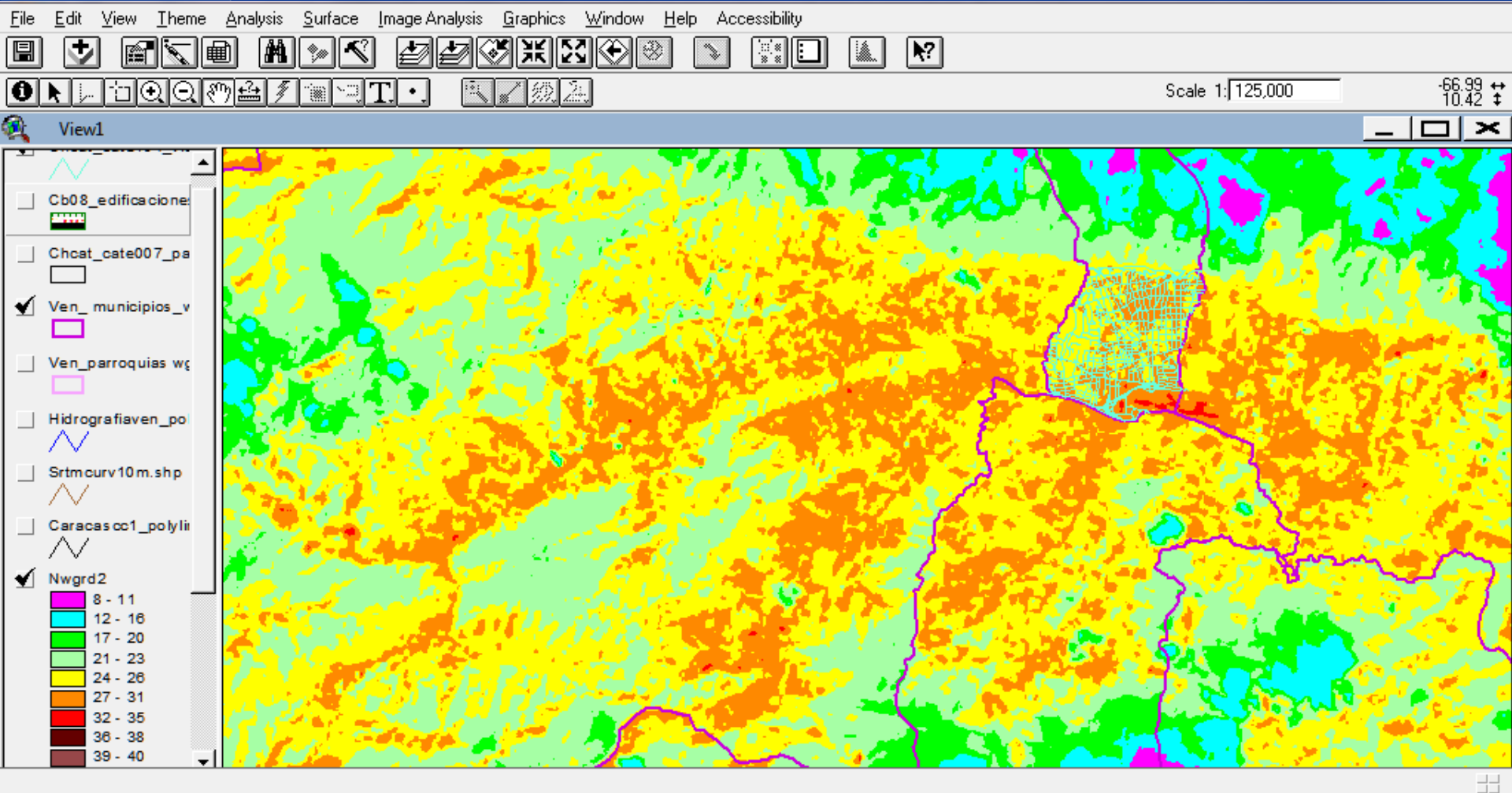


(a)

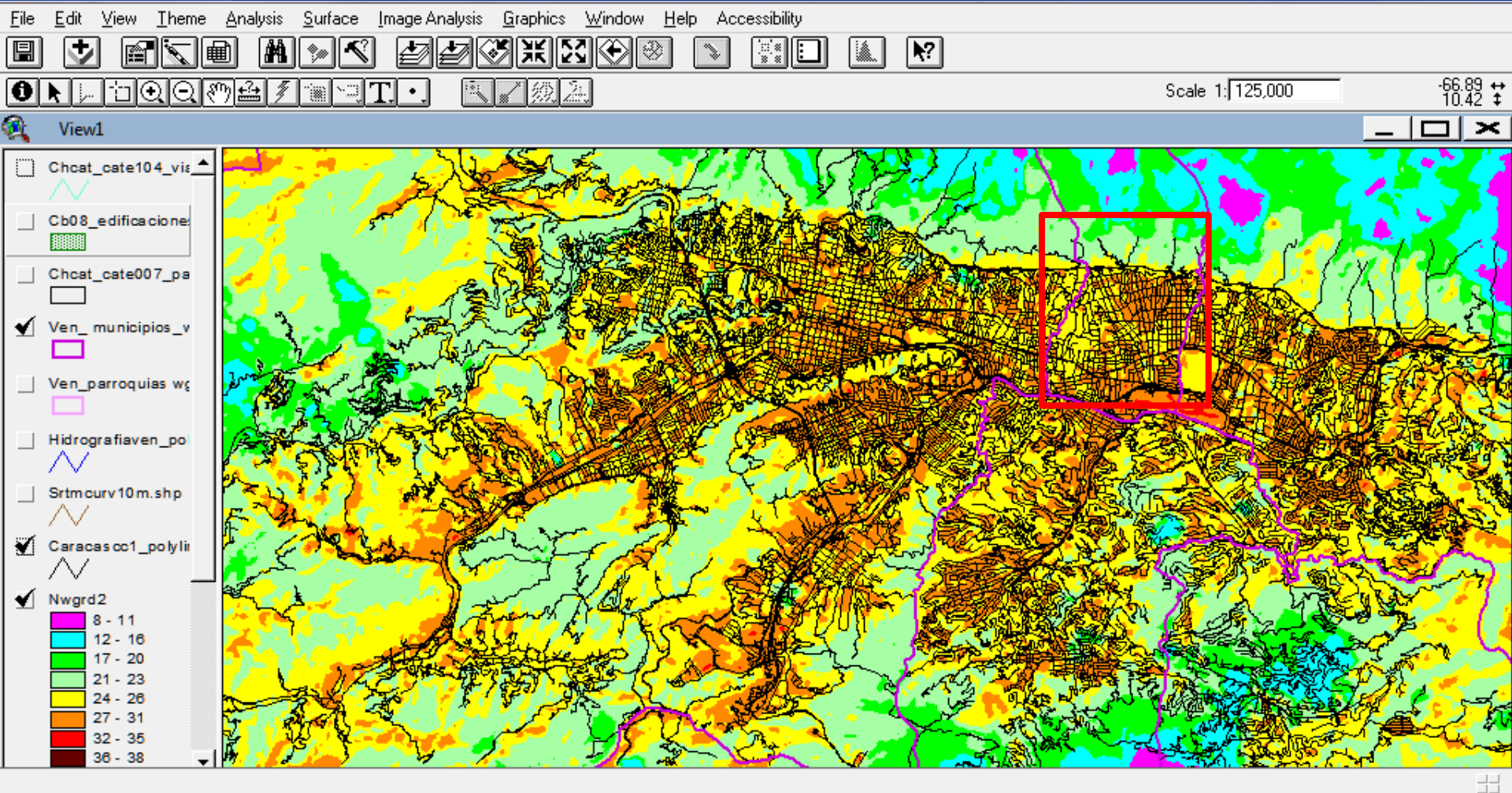


(b)

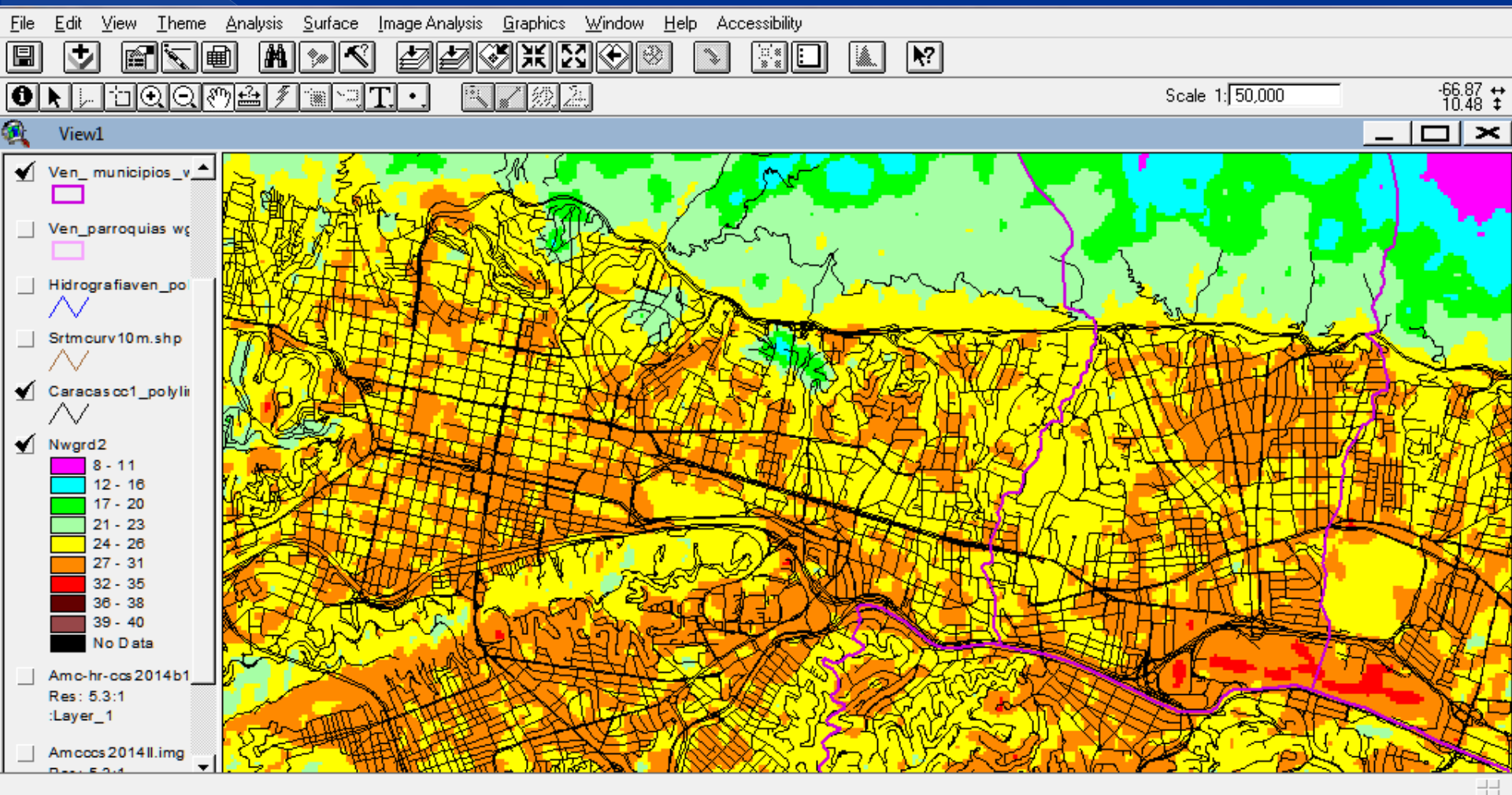
Caracas city. Land surface temperatures patterns + municipalities limits



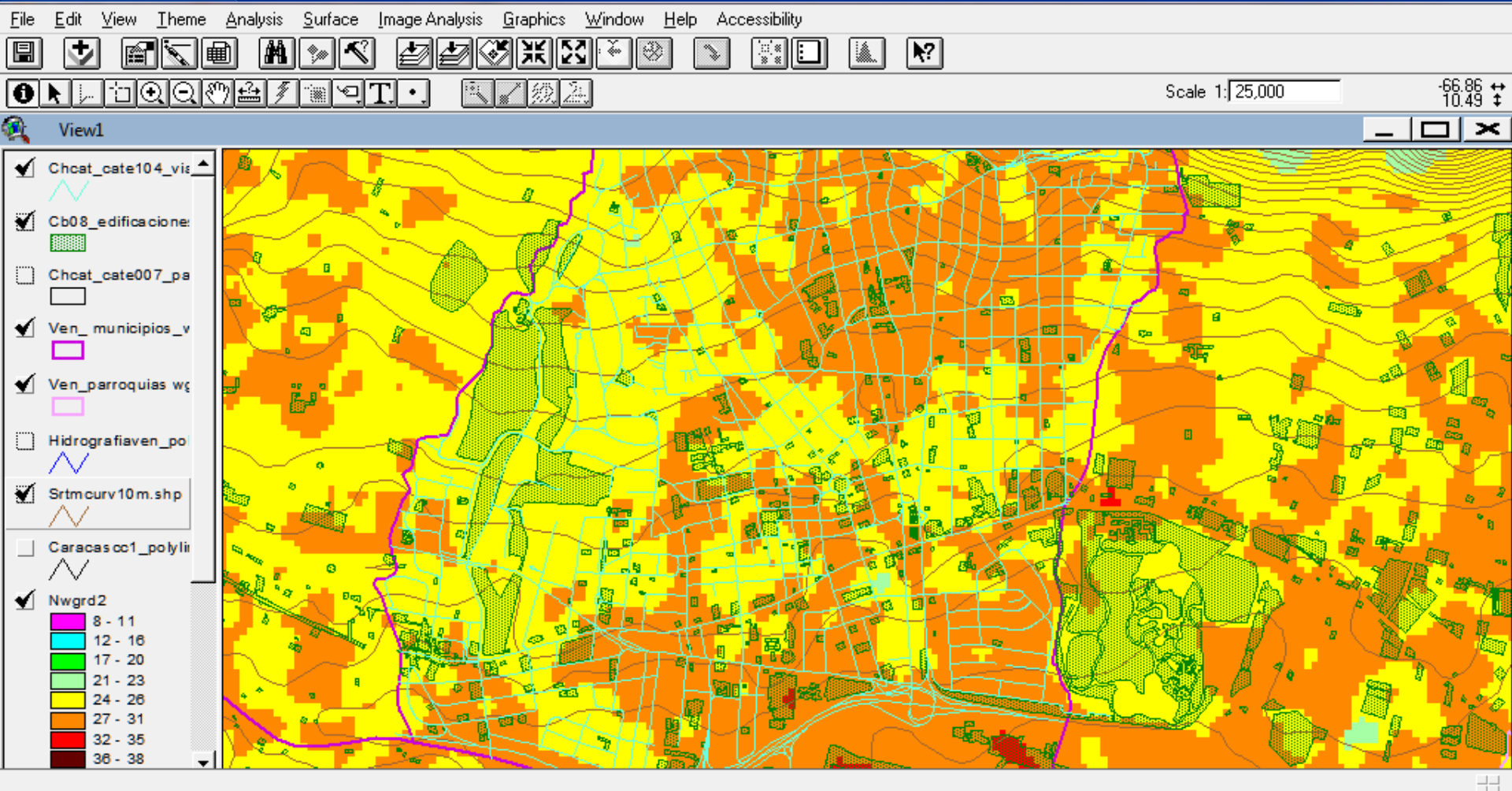
Caracas city. Land surface temperatures patterns + municipalities limits+ streets, roads.



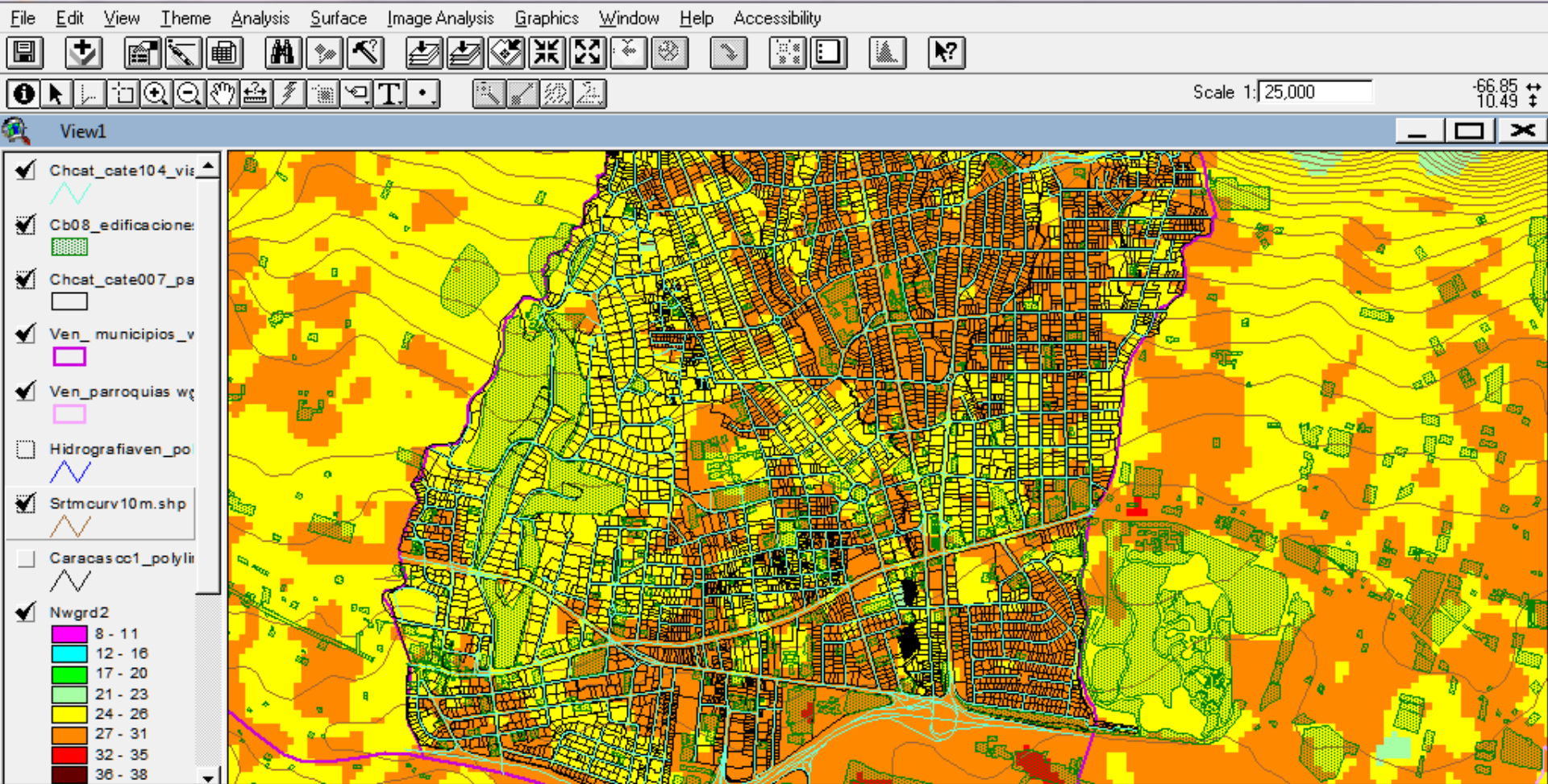
Caracas city. North area. Land surface temperatures patterns + municipalities limits+ streets, roads.



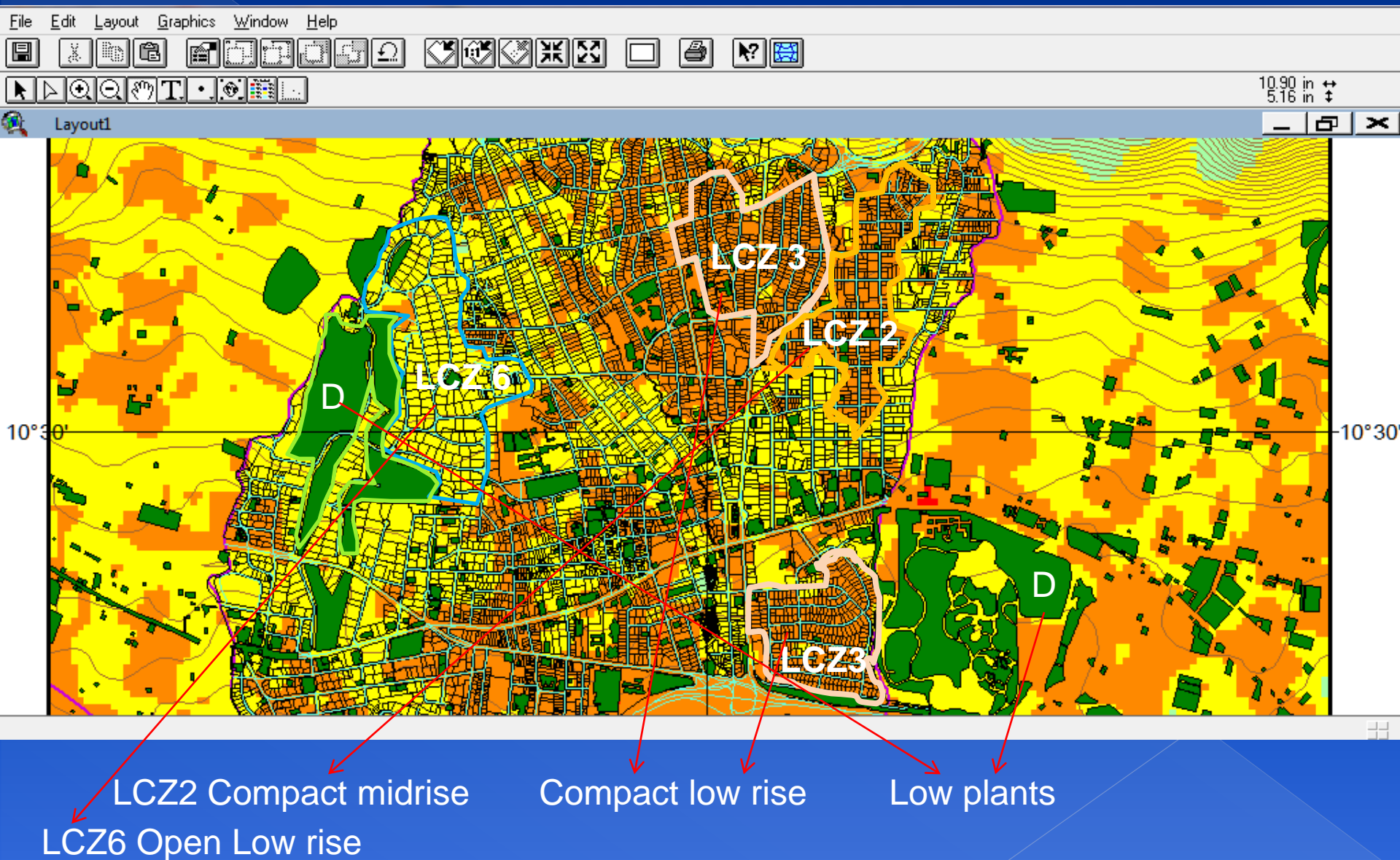
Chacao Municipality: Local surface temperature patterns



Chacao Municipality: Local surface temperature patterns + Roughness



Chacao Municipality: Local surface temperature patterns helps to define LCZs





“Spatial Geotechnologies and GIS tools for urban planners applied to the analysis of urban heat island. Case Caracas city, Venezuela” Contribution 115. GD8: New remote sensing Technology and data

3.3 Conclusions:

- ❖ Integration of GIS data with remotely sensed imagery has increased interest because increased data availability, quality, and decreased data costs across large study extents.
- ❖ This methodology, also demonstrated the potential of data integration/fusion, for urban change mapping.
- ❖ In urban heat island studies, downscaling techniques combine with layers of roads, streets, buildings, into a GIS, can help to explain the differences in urban surface temperatures patterns, medium spatial resolution is been used more frequently in urban heat island and urban climate analysis.



“Spatial Geotechnologies and GIS tools for urban planners applied to the analysis of urban heat island. Case Caracas city, Venezuela” Contribution 115. GD8: New remote sensing Technology and data

References.

- Barsi, Julia A.; Schott, John R.; Hook, Simon J.; Raqueno, Nina G.; Markham, Brian L.; Radocinski, Robert G., (2014). Landsat-8 Thermal Infrared Sensor (TIRS) Vicarious Radiometric Calibration. *Remote Sens.* 6, no. 11: 11607-11626.
- Chander, G., & Markham, B. (2003). Revised Landsat-5 TM radiometric calibration procedures and postcalibration dynamic ranges. *Geoscience and Remote Sensing, IEEE Transactions on*, 41(11), 2674-2677.
- Cordova, Karenia (2011). Urban Climate News. ISSUE N^o. 39 MARCH 2011. Online: <http://urban-climate.com/wp3/wp-content/uploads/2011/04/IAUC039.pdf>
- Cristóbal, J.; Ninyerola, M.; Pons, X. Modeling air temperature through a combination of remote sensing and GIS data. *J. Geophys. Res.* 2008, 113, doi:10.1029/2007JD009318.
- Jimenez-Munoz, J. C., Sobrino, J., Skokovic, D., Mattar, C., & Cristobal, J. (2014). Land surface temperature retrieval methods from Landsat-8 thermal infrared sensor data. *Geoscience and Remote Sensing Letters, IEEE*, 11(10), 1840-1843.
- Rogan, J., Miller, J., Wulder, M. A., & Franklin, S. E. (2006). Integrating GIS and remotely sensed data for mapping forest disturbance and change. *Understanding forest disturbance and spatial pattern: remote sensing and GIS approaches*, 133-172.
- Rozenstein, O.; Qin, Z.; Derimian, Y.; Karnieli, A (2014). Derivation of land surface temperature for Landsat-8 TIRS using a split window algorithm. *Sensors* 14, 5768–5780.
- U.S.Geological Survey (2015) LANDSAT 8 (L8) DATA USERS HANDBOOK, Version 1.0, June, 2015. online: <http://landsat.usgs.gov/documents/Landsat8DataUsersHandbook.pdf>
- Voogt, J. A., & Oke, T. R. (2003). Thermal remote sensing of urban climates. *Remote sensing of environment*, 86(3), 370-384.
- Wang, F., Qin, Z., Song, C., Tu, L., Karnieli, A., & Zhao, S. (2015). An Improved Mono-Window Algorithm for Land Surface Temperature Retrieval from Landsat 8 Thermal Infrared Sensor Data. *Remote Sensing*, 7(4), 4268-4289.
- Yu, X., Guo, X., & Wu, Z. (2014). Land Surface Temperature Retrieval from Landsat 8 TIRS—Comparison between Radiative Transfer Equation-Based Method, Split Window Algorithm and Single Channel Method. *Remote Sensing*, 6(10), 9829-9852.

**Thank You So Much
by your attention**



Dra. Karenia Córdova Sáez.
Profa. Investigadora del
Instituto de Geografía y
Desarrollo Regional,
IGDR /FHE /UCV
kareniac@gmail.com